

Effect of Particle Size on Mechanical Properties of Epoxy Resin Filled with Angular-Shaped Silica

YOSHINOBU NAKAMURA,*¹ MIHO YAMAGUCHI,¹ MASAYOSHI OKUBO,² and TSUNETAKA MATSUMOTO²

¹Central Research Laboratory, Nitto Denko Corp., Shimohozumi, Ibaraki, Osaka 567, Japan, and ²Department of Industrial Chemistry, Faculty of Engineering, Kobe University, Nada-ku, Kobe 657, Japan

SYNOPSIS

Effect of particle size on the mechanical properties of cured epoxy resins has been studied. Resin was filled with angular-shaped silica particles prepared by crushing fused natural raw quartz. These particles were sorted into six groups having different mean sizes ranging from 2–47 μm . Flexural and compressive moduli of the cured epoxy resin slightly decreased with decrease in the particle size of the silica, whereas tensile modulus slightly increased. Flexural and tensile strengths increased with decrease in particle size. Fractured surfaces were observed using scanning electron microscopy to clarify the initiation point of fracture.

INTRODUCTION

In a series of our investigations,^{1–7} the effects of the morphology of cured epoxy resin with a two-phase structure on its properties were studied.

To reduce the internal stress generated by shrinkage in the cooling process from cure temperature to room temperature, soft polymer particles were dispersed as domains (second phase) in the epoxy matrix.^{1–6} The relationship between the morphology of this epoxy resin modified with acrylic polymers and the internal stress has been studied. As a result, it was clarified that the internal stress was effectively reduced by decreasing the domain size¹ and further by introducing a strong interaction at the domain/matrix interface.^{2–6}

To improve the poor resistance to crack propagation, rigid filler particles as a second phase were added to the epoxy resin.⁷ For this study, angular-shaped silica particles prepared by crushing fused natural raw silica were sorted into six groups having different mean sizes ranging from 2–47 μm . Recently, the cured epoxy resin filled with this type of silica particles were used as packaging material for integrated circuits.^{8,9} The effect of particle size on the fracture toughness of cured epoxy resin filled with these particles has been studied. It was noted

that the critical stress intensity factor increased with particle size. The crack tip regions were observed by a scanning electron microscope (SEM) to evaluate the toughening mechanism obtained by increasing size.

In this study, the effect of particle size on mechanical properties such as Young's modulus and mechanical strength was investigated using the same silica particles.

EXPERIMENTAL

Materials

Angular-shaped silica particles were prepared by crushing amorphous silica, made by fusing natural raw quartz at 1,900°C (RD-8, Tatsumori Ltd.). Crushed particles were sorted into six groups by air separation. As shown in a previous article,⁷ the particle size at which the accumulated distribution values reached 50% were defined as the mean particle sizes. The mean sizes of the particle classifications were 2, 5, 13, 18, 33, and 47 μm . The specific surface area of each silica particle was measured according to BET equation using a gas adsorption apparatus (Flow Sorb II 2300, Shimazu Corp.).

Epoxy resin used was bisphenol-A (Epikote 828, Shell Chemical Co., equivalent weight per epoxy group: 190 ± 5 , average molecular weight: 380). 1,2-Cyclohexanedicarboxylic anhydride was used as a

* To whom correspondence should be addressed.

hardner and tri-*n*-butylamine was used as an accelerator for curing of the epoxy resin.

Sample Preparation

Silica particles [204 or 296 parts per hundred resin (phr) by weight) were dispersed in the mixture of the epoxy resin (100 phr) and the hardner (66 phr) by stirring at room temperature for 1 h under vacuum. The accelerator (0.5 phr) was added to the mixture and stirred for 10 min. The final mixture was cured in a mold [4×10 , height: 100 mm, 15×15 , height: 100 mm, and dumb-bell type as shown in Figure 1(b)] at 120°C for 2 h, followed by 140°C for 21 h.

Mechanical Test

Mechanical properties of the cured epoxy resin filled with silica particles were measured by three different modes as follows.

Flexural Test

The shape and dimension of the three-point bend flexural test specimen employed in this study are shown in Figure 1(a). The load–time curve was recorded using tensile testing machine (Tensilon UTM-5T, Orientec Corp.) at a displacement rate of 5 mm/min at room temperature. The load–time curve is schematically shown in the upper part of Figure 1(a).

The flexural modulus (E_f) and the flexural strength (σ_f) were calculated from following equations (ASTM D790):

$$E_f = \frac{S^3}{4B \cdot W^2} \cdot m \quad (1)$$

$$\sigma_f = \frac{3P_c \cdot S}{2W \cdot B^2}, \quad (2)$$

where P_c is the load at specimen break, W is the specimen width, B is the specimen thickness, S is the support span, and m is the slope of the tangent to the initial straight-line portion of the load–time curve as shown in Figure 1(a). The displacement at break value is shown as Δl in Figure 1(a).

Tensile Test

Shape and dimension of the tensile test specimen (dumb-bell shaped type) employed in this study are shown in Figure 1(b). An extensometer ($L_0 = 50$ mm) was attached to the center part of the specimen. The load–displacement curve was recorded using the same method as the flexural test.

The tensile modulus (E_t) and tensile strength (σ_t) were calculated from following equations:

$$E_t = \frac{P/A}{\Delta L/L_0} \quad (3)$$

$$\sigma_t = \frac{P_c}{A}, \quad (4)$$

where $\Delta L/L_0$ is the degree of sample elongation, $P/\Delta L/L_0$ is a slope of the tangent to the initial straight-line portion of the load–displacement curve, and A is the cross-sectional area for the dumb-bell specimen.

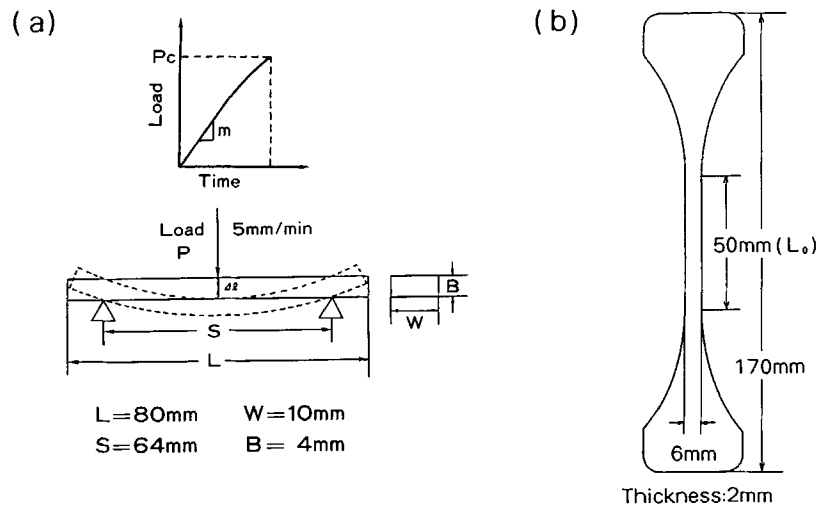


Figure 1 Shape and dimension of mechanical test specimens. (a), flexural test; (b), tensile test.

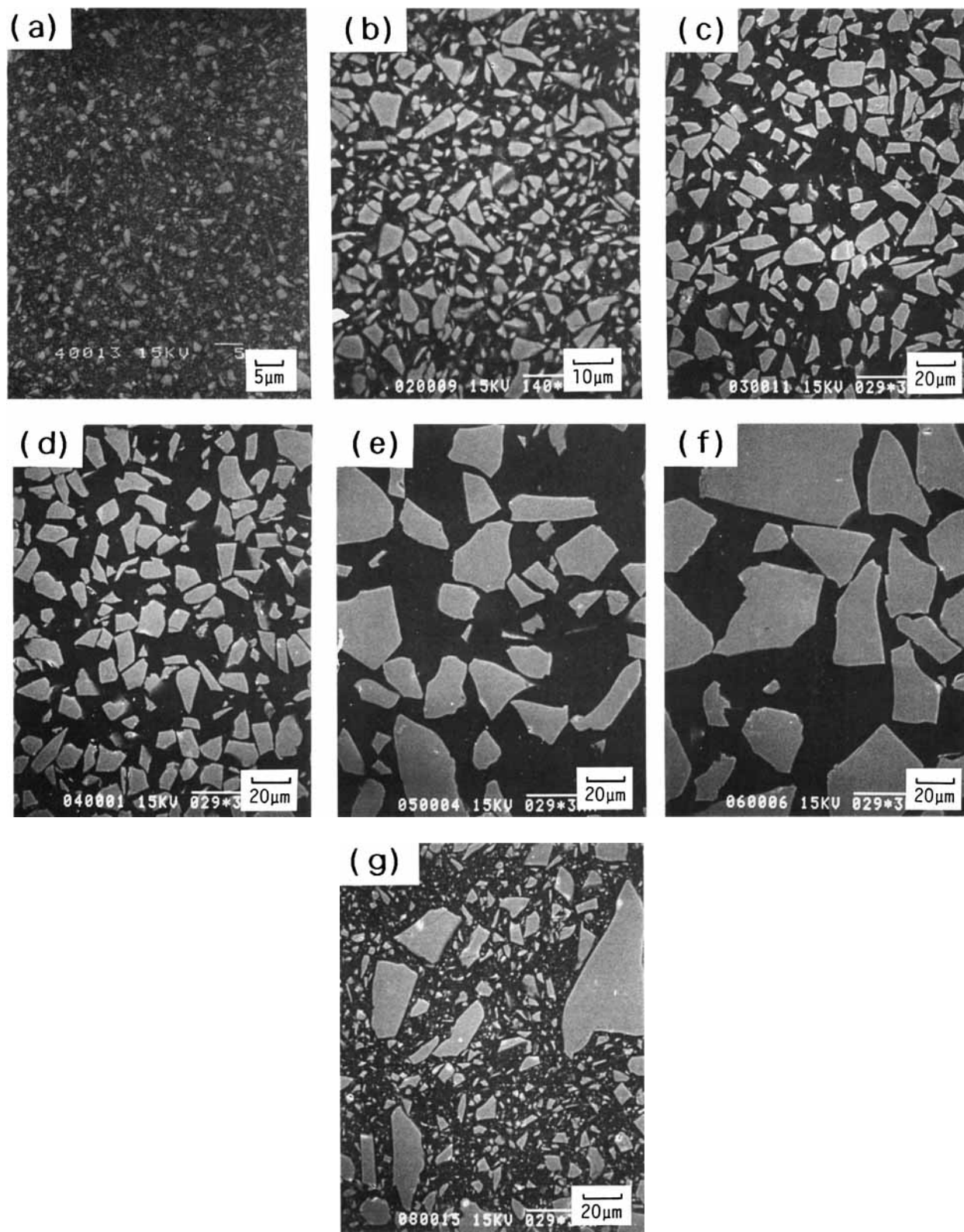


Figure 2 SEM photographs of polished surfaces of cured epoxy resins filled with sorted (a-f) and unsorted original (g) angular-shaped silica particles with a particle content of 55 wt %. Mean particle size of filled silica: (a), 2 μm; (b), 5 μm; (c), 13 μm; (d), 18 μm; (e), 33 μm; (f), 47 μm; (g), 16 μm.

Compressive Test

The compressive test was carried out using the specimen with the size of $15 \times 15 \times 15$ mm. The load-time curve was recorded and compressive modulus (E_c) was calculated from eq. (3).

RESULTS AND DISCUSSIONS

Figure 2 shows SEM photographs for the polished surfaces of cured epoxy resins filled with sorted (a-f) and unsorted original (g) angular-shaped silica particles with a particle content of 55 wt %. These photographs indicate that the particles in each sample were well dispersed in the matrix. Only in the largest particle-filled resin (f) did the concentration of particles slightly increase from top to bottom of the mold due to sedimentation of particles during curing. However, even in that case, since particle contents of the fractured part measured were almost equal to the particle contents in corresponding specimens, influence of the sedimentation was negligible.

Figures 3-5 show the effects of particle content and particle size on the flexural, tensile, and compressive moduli, respectively. The three types of moduli increased with an increase in particle content. Flexural and compressive moduli slightly increased with an increase in the particle size, whereas the tensile modulus slightly decreased. Further, the values measured for the cured epoxy resin filled with

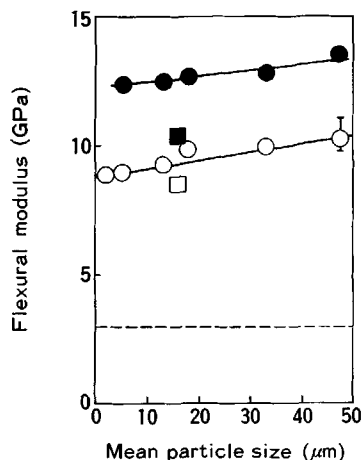


Figure 3 Effect of particle size on flexural modulus of cured epoxy resins filled with unsorted original (□, ■) and sorted (○, ●) angular-shaped silica particles with particle contents of 55 (□, ○) and 64 wt % (■, ●). The broken line indicates the flexural modulus value for unfilled cured epoxy resin.

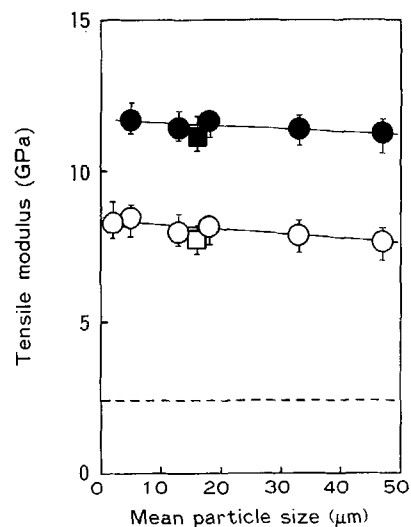


Figure 4 Effect of particle size on tensile modulus of cured epoxy resins filled with unsorted original (□, ■) and sorted (○, ●) angular-shaped silica particles with particle contents of 55 (□, ○) and 64 wt % (■, ●). The broken line indicates the tensile modulus value for unfilled cured epoxy resin.

the unsorted original particles (□, ■) were relatively lower than those filled with the sorted particles (○, ●) in the flexural (Fig. 3) and compressive moduli (Fig. 5), whereas they were similar level in the ten-

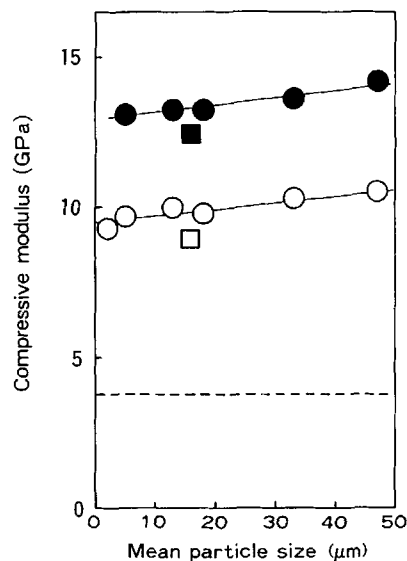


Figure 5 Effect of particle size on compressive modulus of cured epoxy resins filled with unsorted original (□, ■) and sorted (○, ●) angular-shaped silica particles with particle contents of 55 (□, ○) and 64 wt % (■, ●). The broken line indicates the compressive modulus value for unfilled cured epoxy resin.

sile modulus (Fig. 4). The measured values were always higher in the order of compressive modulus > flexural modulus > tensile modulus.

The silica particles used in this study were prepared by crushing fused raw silica. Therefore, when increasing particle size the particles were more densely filled with a narrow distance between particles in the epoxy matrix (see Fig. 2) because its shape became more irregular. As a result, the compressive modulus should be affected by the Young's modulus of own silica particles, and the influence should increase with the particle size. This seems to be the reason that the flexural and compressive moduli were larger than the tensile modulus and the flexural and compressive moduli slightly increased with the particle size. In the cured epoxy resins filled with the unsorted original particles, it was observed that the relative distance between particles was wider than that filled with sorted particles (Fig. 2). This seems to be the reason that the flexural and compressive moduli of the unsorted systems were lower than those of sorted systems. During the flexural test, as shown in Figure 1, the upper part of the specimen is in a compressive mode, whereas the lower part is in a tensile mode. Thus, the flexural modulus shown in Figure 3 seems to be strongly influenced by the compressive mode. A detailed discussion of this phenomena will be reported in a future article in comparison with spherical silica.

Figures 6-8 show the effects of particle size on

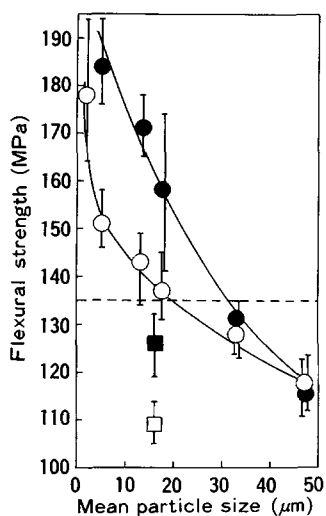


Figure 6 Effect of particle size on flexural strength of cured epoxy resins filled with unsorted original (□, ■) and sorted (○, ●) angular-shaped silica particles with particle contents of 55 (□, ○) and 64 wt % (■, ●). The broken line indicates the flexural strength value for un-filled cured epoxy resin.

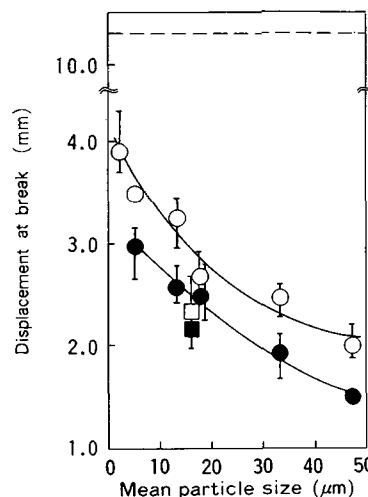


Figure 7 Effect of particle size on displacement at break of cured epoxy resins filled with unsorted original (□, ■) and sorted (○, ●) angular-shaped silica particles with particle contents of 55 (□, ○) and 64 wt % (■, ●) measured by flexural test. The broken line indicates the displacement at break value for un-filled cured epoxy resin.

flexural strength, displacement at break in flexural test, and tensile strength, respectively. These values strongly increased with a decrease in the particle size. Their phenomena were in accordance with those reported by Roulin-Moloney et al.¹⁰ using larger angular-shaped silica particles (mean size: 60-300 μm).

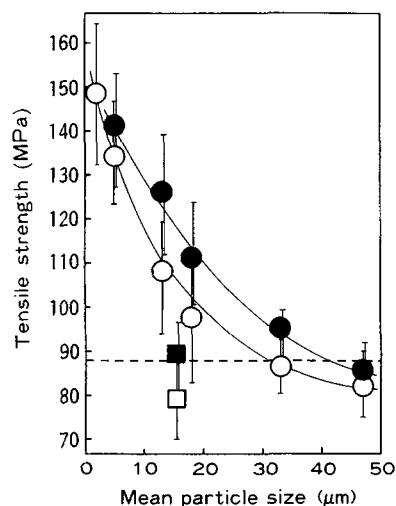


Figure 8 Effect of particle size on tensile strength of cured epoxy resins filled with unsorted original (□, ■) and sorted (○, ●) angular-shaped silica particles with particle contents of 55 (□, ○) and 64 wt % (■, ●). The broken line indicates the tensile strength value for un-filled cured epoxy resin.

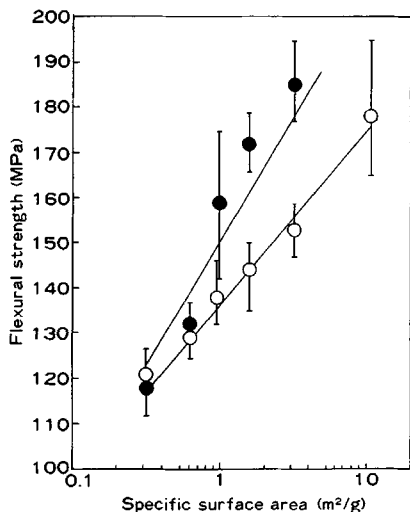


Figure 9 Flexural strength of cured epoxy resins filled with angular-shaped silica particles having different mean sizes with particle contents of 55 (○) and 64 wt % (●) vs. specific surface area of filled silica particles.

Figure 9 shows the relationship between flexural strength value and the specific surface area of filled silica particles. The good relationship between both values indicates that increasing the specific surface area of filled particles increases their mechanical strength. Similar results were obtained in the tensile strength.

Roulin-Moloney et al.¹¹⁻¹⁴ observed the fractured surfaces of the mechanical test specimens of unfilled and filled cured epoxy resins and described that the observation often called “fractography”¹⁴ is useful for clarifying the fracture mechanism. In their observation, the initiation point of fracture for the unfilled resin was surrounded by a small semicircular zone termed “the mirror zone.” This zone was surrounded by a zone termed “the smooth zone,” characterized by “parabolic marks,” and the outside was a zone termed “the rough zone.” In the filled resin, a zone termed “the debonded zone” replaced the mirror zone.

Figure 10 shows SEM photographs of the fractured surfaces of the flexural specimens in this experiment. In all fractured specimens, the fracture initiated on the lower part of specimen (region under tension). Above-mentioned zones were observed in both unfilled (a) and filled (b-d) resins, although they were not as clear as Roulin-Moloney’s results.¹³ Next, the region around the initiation point of fracture was magnified to clarify the effect of particle size on their initiation mechanism of fracture.

Figure 11(a) shows that the initiation point of fracture in the unfilled cured epoxy resin was a defect

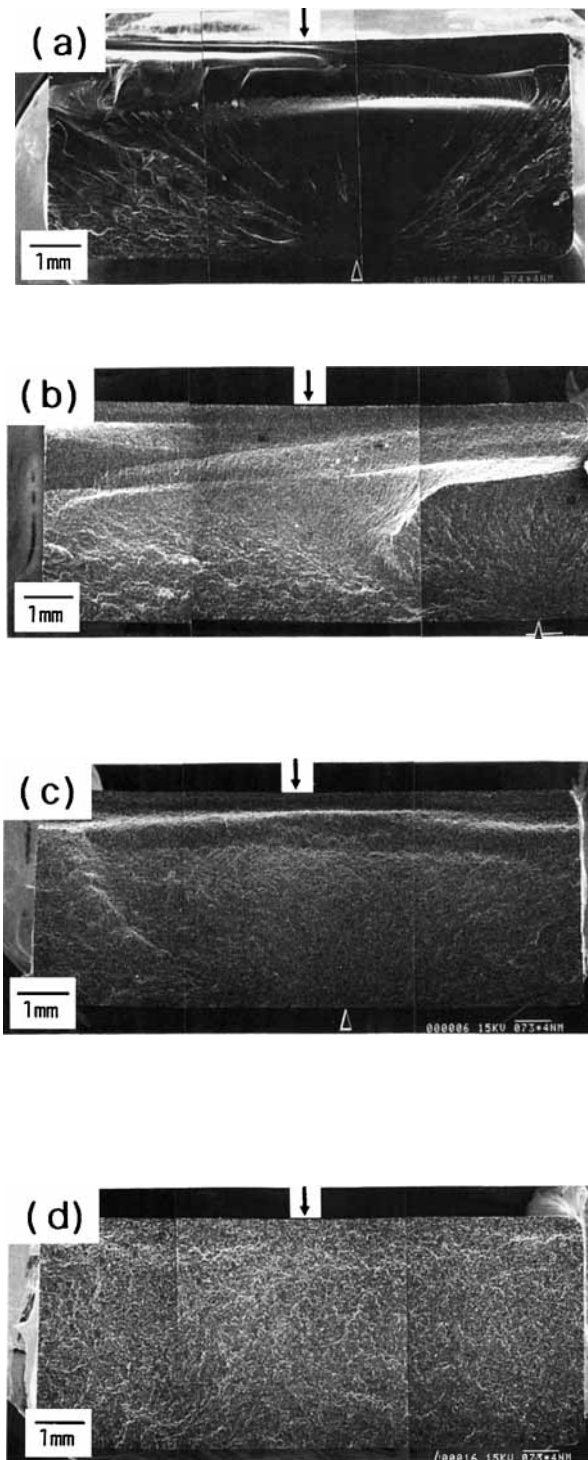


Figure 10 Fractured surfaces for flexural test specimens of unfilled cured epoxy resin (a) and those filled with angular-shaped silica particles (b-d) with a particle content of 64 wt % observed by SEM. Mean particle size of filled silica: (b), 5 μm; (c), 18 μm; (d), 47 μm. The arrow indicates the direction of applied load and triangle mark indicates the initiation point of fracture.

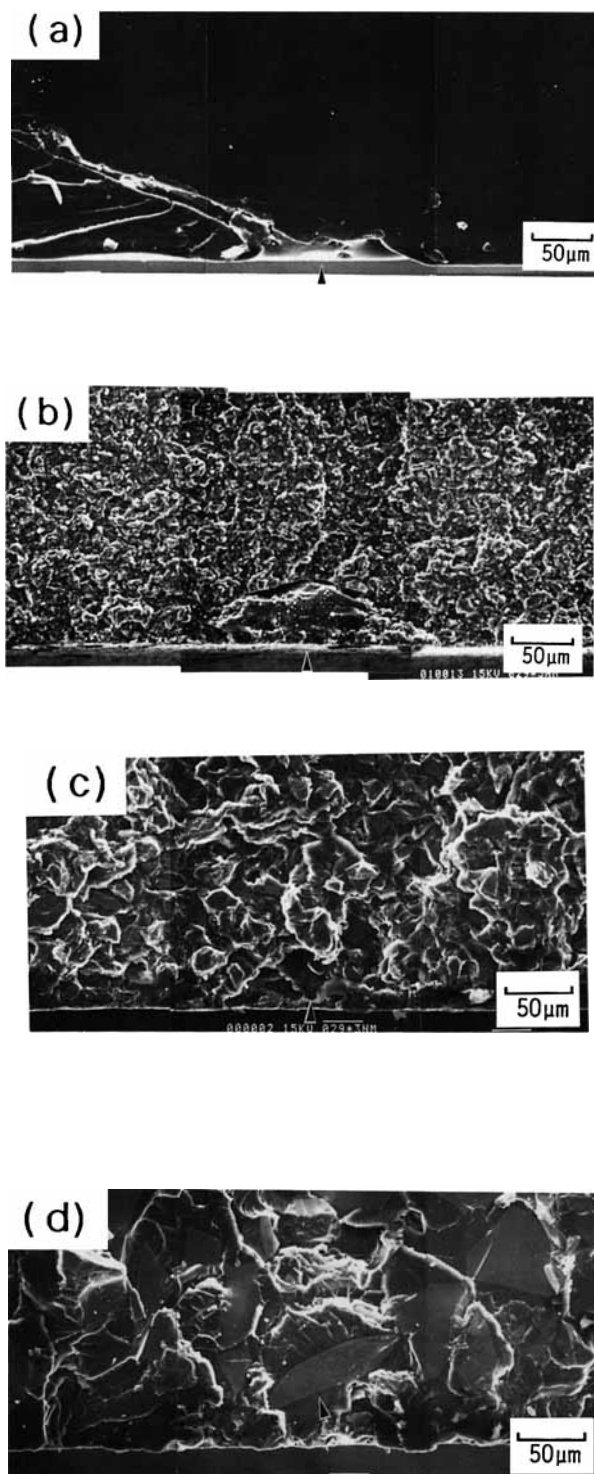


Figure 11 Regions around the initiation point of fracture for fractured flexural test specimens of unfilled cured epoxy resin (a) and those filled with angular-shaped silica particles (b–d) with a particle content of 64 wt % observed by SEM. Mean particle size of filled silica: (b), 5 μm ; (c), 18 μm ; (d), 47 μm . The triangle mark indicates the initiation point of fracture.

on the specimen surface. Figure 11(b) shows a foreign material that had strayed into the specimen during sample preparation in the cured epoxy resin filled with small particles (mean size: 5 μm). The fracture appears to have initiated at the surface of inclusion. In all tested specimens for the unfilled cured epoxy resin and those filled with a mean particle size of 2 and 5 μm particles in mean size, the similar observations in Figures 11(a) and (b) were obtained, whereas with particle sizes greater than 5 μm the fracture initiation point was due to the particle fracture increase [Figs. 11(c) and (d), mean size: 18 and 47 μm , respectively]. In resins filled with mean particle sizes of 33 and 47 μm , the fracture was initiated from particle fracture in all tested specimens. Since the silica particles used in this study were prepared by crushing raw quartz, their shape became more irregular (Fig. 2) and the number of microcracks contained in the particles may increase with increasing particle size. The large particles seem to be easily cracked when the load is applied. Actually, in the previous article⁷ it was clearly shown by SEM observation that the large particles at the crack tip region were cracked easily by concentrated stress during the fracture toughness test, although the small particles were never cracked. These cracked large particles seem to act as the inherent flaw of fracture in the flexural and tensile tests in this article.

The effective inherent flaw size that acts as the source of fracture in the specimen was calculated from the following equation suggested by Roulin-Moloney et al.^{13,14}:

$$K_c = \sigma_t Y \sqrt{a_i}, \quad (5)$$

where K_c is the critical stress intensity factor measured by a single-edge notched beam loaded in the three-point bending (SENB) test, σ_t is the tensile strength, Y is a geometric factor (= 1.99 used), and a_i is the effective inherent flaw size. K_c values used were those measured using SENB test in the previous article.⁷

Table I shows the calculated effective inherent flaw sizes. The mean and maximum particle size values were evaluated from the size distribution curve using laser beam type size distribution analyzer as shown in the previous article.⁷ The calculated flaw sizes increased with increase in the particle size. These results support the above-mentioned view. However, the calculated flaw sizes were relatively larger than their evaluated maximum particle size values. The reason will be discussed in a future article.

Table I Calculated Effective Inherent Flaw Size of Cured Epoxy Resins Filled with Angular-Shaped Silica Particles

Filled Silica Particle					
Mean Size (μm)	Max. Size (μm)	Particle Content (wt %)	σ_t^a (MPa)	K_c^b (MPa $\sqrt{\text{m}}$)	a_i^c (μm)
—	—	0	88	0.78	20
2	-8	55	149	1.40	22
5	-12	55	135	1.90	50
13	-32	55	108	2.05	91
18	-64	55	98	2.28	137
33	-96	55	86	2.27	176
47	-192	55	82	2.76	286
16 ^d	-192	55	79	1.99	160
5	-12	64	142	1.97	49
13	-32	64	126	2.43	94
18	-64	64	112	2.54	130
33	-96	64	96	2.58	182
47	-192	64	85	2.88	289
16 ^d	-192	64	89	2.36	178

^a Tensile strength.

^b Critical stress intensity factor measured by SENB method.

^c Effective inherent flaw size calculated from $K_c = \sigma_t Y \sqrt{a_i}$, where Y is geometric factor (=1.99 used).

^d Unsorted original silica particles.

From above results, it was concluded that the fracture of particles initiated the fracture in the mechanical test and lowered the flexural and tensile strength. In addition to size, shape may also affect mechanical properties. In the above results, however, it is difficult to distinguish between the effects of size and shape on mechanical properties. In a future article, the effect of particle size on the mechanical properties will be discussed using spherical silica particles.

The authors are grateful to Tatsumori Ltd. for preparation of sample silica particles.

REFERENCES

1. Y. Nakamura, H. Tabata, H. Suzuki, K. Iko, M. Okubo, and T. Matsumoto, *J. Appl. Polym. Sci.*, **32**, 4865 (1986).
2. Y. Nakamura, H. Tabata, H. Suzuki, K. Iko, M. Okubo, and T. Matsumoto, *J. Appl. Polym. Sci.*, **33**, 885 (1987).
3. Y. Nakamura, M. Yamaguchi, A. Kitayama, K. Iko, M. Okubo, and T. Matsumoto, *J. Appl. Polym. Sci.*, **39**, 1045 (1990).
4. Y. Nakamura, M. Yamaguchi, K. Iko, M. Okubo, and T. Matsumoto, *J. Mater. Sci.*, **25**, 2711 (1990).
5. Y. Nakamura, M. Yamaguchi, K. Iko, M. Okubo, and T. Matsumoto, *Polymer*, **31**, 2066 (1990).
6. Y. Nakamura, M. Yamaguchi, K. Iko, M. Okubo, and T. Matsumoto, *Kobunshi Ronbunshu*, **47**, 277 (1990).
7. Y. Nakamura, M. Yamaguchi, A. Kitayama, M. Okubo, and T. Matsumoto, *Polymer*, to appear.
8. N. Kinjo, M. Ogata, K. Nishi, and A. Kaneda, *Adv. Polym. Sci.*, **88**, 1 (1989).
9. A. Nishimura, A. Tatemichi, H. Miura, and T. Sakamoto, *IEEE Trans. Components, Hybrids, Manuf. Technol.*, **CHMT-12**(4), 637 (1987).
10. A. C. Roulin-Moloney, W. J. Cantwell, and H. H. Kausch, *Polym. Compos.*, **8**, 314 (1987).
11. A. C. Moloney, H. H. Kausch, and H. R. Stieger, *J. Mater. Sci.*, **18**, 208 (1983).
12. A. C. Moloney, H. H. Kausch, T. Kaiser, and H. R. Beer, *J. Mater. Sci.*, **22**, 381 (1987).
13. W. J. Cantwell, A. C. Roulin-Moloney, and T. Kaiser, *J. Mater. Sci.*, **23**, 1615 (1988).
14. A. C. Roulin-Moloney (ed.), *Fractography and Failure Mechanisms of Polymers and Composites*, Elsevier Applied Science, London and New York, 1988.

Received August 27, 1990

Accepted February 4, 1991